Video Article

Stereolithographic 3D Printing with Renewable Acrylates

Vincent S.D. Voet[1], Geraldine H.M. Schnelting[1], Jin Xu[2], Katja Loos[2], Rudy Folkersma[1], Jan Jager[1]

[1]Professorship Sustainable Polymers, NHL Stenden University of Applied Sciences

[2]Macromolecular Chemistry and New Polymeric Materials, Zernike Institute for Advanced Materials, University of Groningen

Correspondence to: Vincent S.D. Voet at vincent.voet@stenden.com

URL: https://www.jove.com/video/58177
DOI: doi:10.3791/58177

Keywords: Chemistry, Issue 139, Additive, Manufacturing, Biobased, Sustainable, Photopolymer, Resin

Date Published: 9/12/2018

Citation: Voet, V.S., Schnelting, G.H., Xu, J., Loos, K., Folkersma, R., Jager, J. Stereolithographic 3D Printing with Renewable Acrylates. *J. Vis. Exp.* (139), e58177, doi:10.3791/58177 (2018).

Abstract

The accessibility of cost-competitive renewable materials and their application in additive manufacturing is essential for an efficient biobased economy. We demonstrate the rapid prototyping of sustainable resins using a stereolithographic 3D printer. Resin formulation takes place by straightforward mixing of biobased acrylate monomers and oligomers with a photoinitiatior and optical absorber. Resin viscosity is controlled by the monomer to oligomer ratio and is determined as a function of shear rate by a rheometer with parallel plate geometry. A stereolithographic apparatus charged with the biobased resins is employed to produce complex shaped prototypes with high accuracy. The products require a post-treatment, including alcohol rinsing and UV irradiation, to ensure complete curing. The high feature resolution and excellent surface finishing of the prototypes is revealed by scanning electron microscopy.

Video Link

The video component of this article can be found at https://www.jove.com/video/58177/

Introduction

Rapid prototyping enables on-demand production and design freedom and allows the efficient manufacturing of 3D constructs in a layer-by-layer manner[1]. As a result, 3D printing as a fabrication technique has developed rapidly in recent years[2]. Various technologies are available, all relying on the translation of virtual models into physical objects, and applying processes such as extrusion, direct energy deposition, powder solidification, sheet lamination and photopolymerization. The latter involves stepwise UV curing of liquid photopolymer resins. In 1986, Hull and co-workers developed the stereolithography apparatus (SLA), a UV laser-based 3D printer. More recently, a similar process called digital light processing (DLP) has become available, in which photopolymerization is initiated by a light projector. Together, DLP and SLA are referred to as stereolithography 3D printing[3].

SLA is applied in high-resolution prototyping and fabrication of biomedical devices[4,5]. This technology is superior to the widely used fused deposition modeling (FDM) in terms of accuracy, surface finishing and resolution[6]. Depending on the architecture of the product, a support structure is integrated in the 3D model to stabilize the construct during fabrication. Furthermore, a post-printing treatment of manufactured parts is required[7,8]. Typically, printed objects are washed in an alcohol bath to dissolve unreacted resin, and subsequent curing in an UV oven is performed to guarantee full conversion of the polymerization[9].

In general, resins for lithography-based additive manufacturing rely on photocurable systems containing multifunctional acrylates or epoxides[10]. Current photopolymer resins on the commercial market are fossil-based and expensive, while the availability of low-cost renewable resins is needed to facilitate waste-free and local manufacturing of sustainable 3D products for a biobased economy[1,6]. Recently, photopolymer resins based on renewable acrylates were developed and successfully applied in stereolithography 3D printing[11,12]. In this detailed protocol, we demonstrate the rapid prototyping with biobased resins on a commercial stereolithography apparatus. Special attention is paid to critical steps in the procedure, *i.e.,* resin formulation and post-printing treatments, to help new practitioners in the field of additive manufacturing.

Protocol

CAUTION: Please consult all relevant material safety data sheets (MSDS) before use.

1. Preparation of Photocurable Resin

NOTE: Please use personal protective equipment (safety glasses, gloves, lab coat) during the following procedure. See our previous work[12] for more details on this section.

1. Pour 50 g of 1,10-decanediol diacrylate (SA5201) in a 500 mL Erlenmeyer flask.

2. Add 1.0 g of diphenyl(2,4,6-trimethylbenzoyl)phosphine oxide (TPO) and 0.40 g of 2,5-*bis*(5-*tert*-butyl-benzoxazol-2-yl)thiophene (BBOT) to the flask.
3. Equip the flask with a mechanical stirrer and stir the mixture at 200 rpm for 5 min at room temperature in order to dissolve TPO and BBOT in the acrylate monomer.
4. Add 100 g of pentaerythritol tetraacrylate and 100 g of multifunctional epoxy acrylate (see **Table of Materials**) to the mixture.
5. Stir the mixture at 200 rpm for 30 min at 50 °C to ensure a homogeneous resin.
6. Remove the mechanical stirrer and fit the flask with a stopper. The flask is wrapped in aluminium foil to protect the biobased acrylate photopolymer resin (BAPR) from light.
   NOTE: The protocol can be paused here.
7. Cover the bottom plate of a rheometer with parallel-plate geometry with the photoresin.
8. Set the gap between the plates at 1 mm and cover the rheometer with a UV resistant hood.
9. Measure the resin viscosity at room temperature at shear rates from 0.1 to 100 s^{-1}; *e.g.,*0.100, 0.126, 0.158, 0.200, 0.251, 0.316, 0.398, 0.501, 0.631, 0.794, 1.00, 1.26, 1.58, 2.00, 2.51, 3.16, 3.98, 5.01, 6.31, 7.94, 10.0, 12.6, 15.8, 20.0, 25.1, 31.6, 39.8, 50.1, 63.1, 79.4, and 100 s^{-1}.

2. Stereolithographic 3D Printing with Biobased Acrylates

NOTE: See our previous work[12] for more details on this section.

1. Turn on the SLA 3D printer and select open mode.
2. Start the model preparation software on a computer. Choose the desired print settings: material (Clear), version (V4) and layer thickness (50 µm).
3. Open the digital model of the complex-shaped prototype, a standard tessellation language (.stl) file (see **Supplemental Coding File**) and choose the location and orientation on the build platform. Upload the print job from the model preparation software to the SLA 3D printer.
   NOTE: Depending on the architecture of the product, a support structure can be integrated in the 3D model to stabilize the construct during fabrication. In case of the complex-shaped prototype demonstrated here, a support structure is not required if printed normal to the build direction.
4. Pour 200 mL of the biobased photoresin into a resin tank. Open the 3D printer and mount the resin tank properly.
5. Mount the build platform and close the 3D printer.
6. Start the print job.
7. Allow the 3D printer to fabricate complex shaped prototypes. Do not open the printer until the print job is finished.
   NOTE: Before printing, make sure the 3D printer is leveled. For the demonstrated protocol, the wavelength of the UV laser is 405 nm. The print time of the object is 2.5 h.

3. Post-treatment of 3D Printed Objects

NOTE: Please use personal protective equipment (safety glasses, gloves) during the following procedure.

1. When the print job is finished, open the printer. Remove the build platform, with the produced parts attached, and close the printer.
2. Open the washing station, filled with isopropyl alcohol, and insert the build platform. Start the procedure and rinse for 20 min to remove any unreacted resin.
3. When the rinsing procedure is finished, remove the build platform from the washing station and detach the prototypes from the build platform.
4. Allow the prototypes to air dry for 30 min. In the meantime, preheat the UV oven at 60 °C.
   NOTE: Preheating will take at least 15 min. The UV wavelength of the oven is 405 nm, identical to the wavelength of the SLA laser.
5. Open the UV oven and quickly place the prototypes on the rotating platform. Close the UV oven and cure for 60 min at 60 °C to ensure complete conversion.
6. When the post-curing procedure is finished, open the UV oven and take out the prototypes.

4. Characterization of Surface Morphology of Complex-shaped Prototypes

NOTE: See our previous work[12] for more details on this section.

1. Cut ca. 1 cm of internal helix from the complex shaped prototype using a razor blade.
2. Attach the sample to the sample holder with double sided carbon conductive tape.
3. Prior to imaging, coat the sample with 30 nm Pt/Pd (80:20) on a sputtering system.
4. Insert the sample into a scanning electron microscope operating at an accelerating voltage of 5 kV. Acquire several images of the sample at 30X and 120X magnification.

Representative Results

Four representative resin compositions are displayed in **Table 1**, along with their average biobased carbon content (BC) derived from the individual BC of the components. The resin viscosity (**Figure 1**) is influenced by the ratio of acrylate monomers and oligomers and typically demonstrates Newtonian behavior. The mechanical properties of parts manufactured from various resins were determined by stress-strain analysis. **Figure 2** displays the representative outcome on a universal testing machine in terms of E-modulus and tensile strength. The effect of the post-printing treatment on the product performance is depicted in **Figure 3**. The smooth surface and high feature resolution of complex shaped prototypes is revealed by the electron microscope (**Figure 4**). The extent of surface cracking is related to the initial resin viscosity.

Resin	TPO	BBOT	SA5102	SA5201	SA5400	SA7101	BC
	% w/w	% w/w	% w/w	% w/w	% w/w	% w/w	%
BAPR-α	0.40	0.16	20	40		40	67
BAPR-β	0.40	0.16		60		40	64
BAPR-γ	0.40	0.16		20	40	40	44
BAPR-δ	0.40	0.16			60	40	34

Table 1: Renewable acrylate resin formulation. Characteristics of representative bioacrylate resins, depicting resin composition and biobased carbon content.

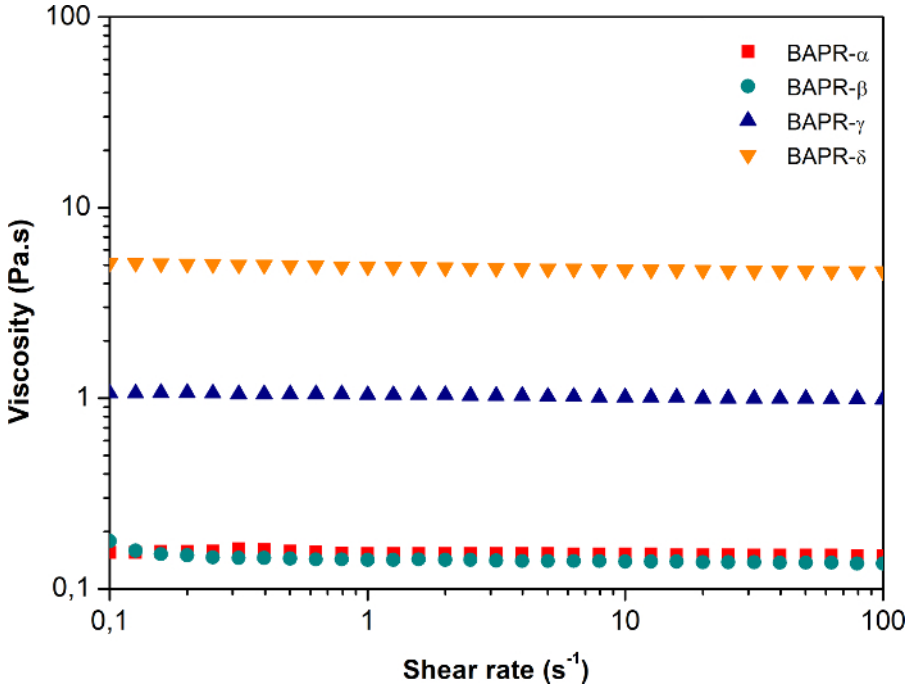

Figure 1: Rheological behavior of renewable acrylate resins prior to 3D printing. Viscosity as a function of shear rate for uncured BAPR samples. Figure is adapted with permission (copyright 2018 American Chemical Society).[12] Please click here to view a larger version of this figure.

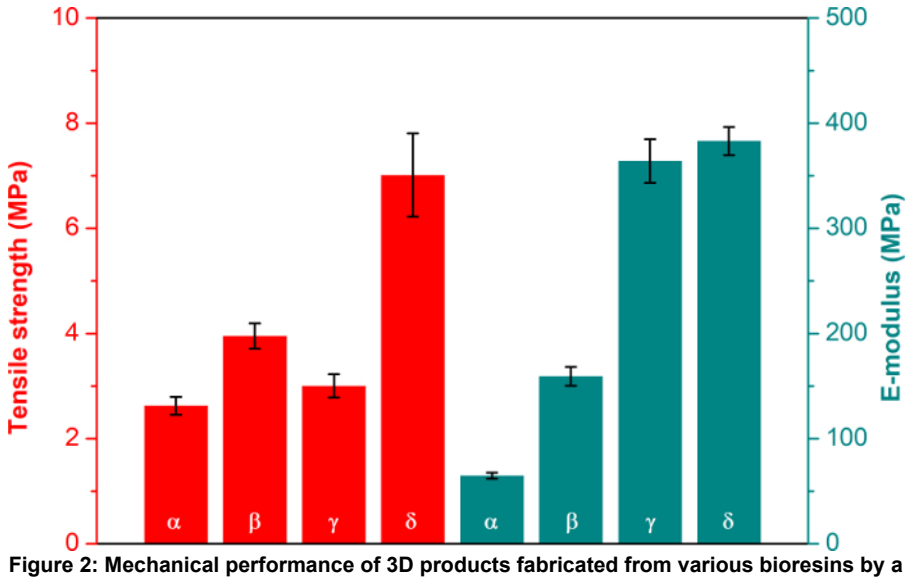

Figure 2: Mechanical performance of 3D products fabricated from various bioresins by a stereolithography apparatus. Tensile strength (red) and Young's modulus (cyan) of produced parts from cured BAPRs. The tensile bars (ISO 527-2-1BA) were printed normal to the build direction. Error bars indicate the standard deviation. Please click here to view a larger version of this figure.

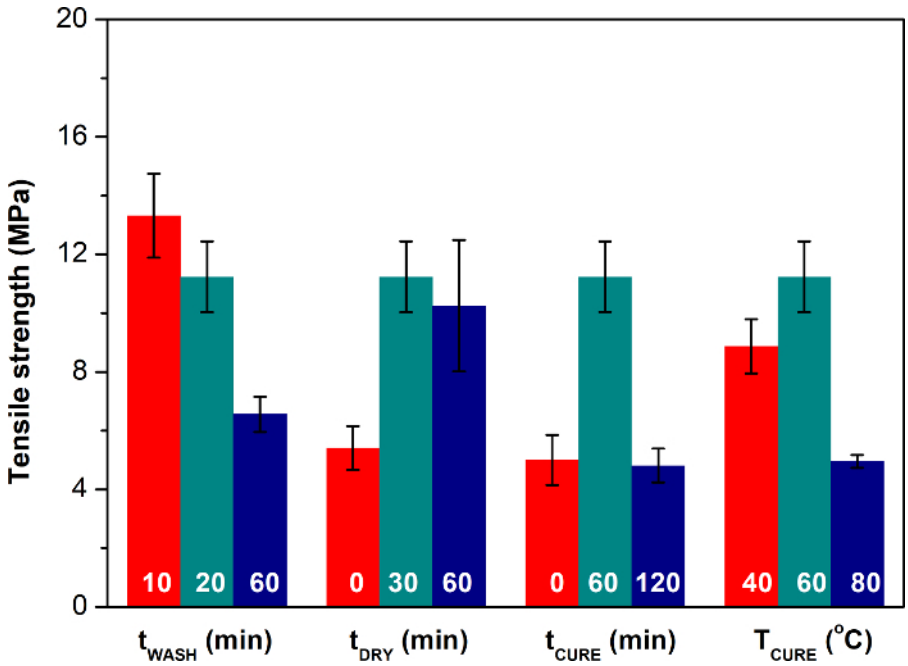

Figure 3: Influence of post-printing treatment on mechanical performance of 3D products. Tensile strength of produced parts post-treated under various conditions. The tensile bars (ISO 527-2-1BA) were printed normal to the build direction. Error bars indicate the standard deviation. Please click here to view a larger version of this figure.

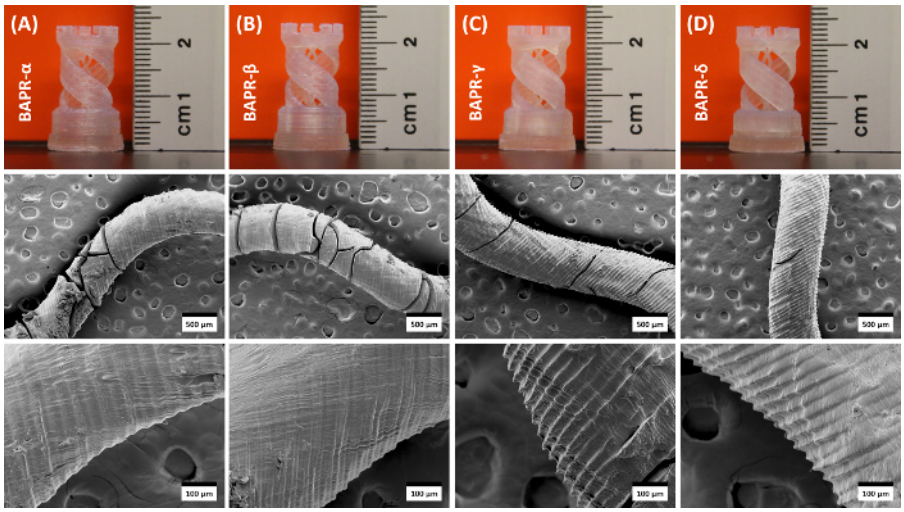

Figure 4: Visual and microscopic representation of complex-shaped prototypes fabricated from various bioresins by a stereolithography apparatus. (A) Photo of rook tower prototype printed with BAPR-α (top) and SEM images of corresponding internal helix (bottom). **(B)** Photo of rook tower prototype printed with BAPR-β (top) and SEM images of corresponding internal helix (bottom). **(C)** Photo of rook tower prototype printed with BAPR-γ (top) and SEM images of corresponding internal helix (bottom). **(D)** Photo of rook tower prototype printed with BAPR-δ (top) and SEM images of corresponding internal helix (bottom). Figure is adapted with permission (copyright 2018 American Chemical Society)[12]. Please click here to view a larger version of this figure.

Discussion

Additive manufacturing is applied in fabrication of tailor-made prototypes and small series, when the higher production costs per part can compete with conventional processes since there is no need for production of molds and tools. In the last decade, the revenues from services and products related to additive manufacturing have grown exponentially[13]. The largest fraction of material sales is from photopolymers. The growth attracted attention and initiated the investments of major industries, *e.g.,* aerospace, automotive, medical. Therefore, the field of 3D printing is expected to further expand in the upcoming years.

We have demonstrated an efficient method for the accurate and on-demand fabrication of sustainable products with renewable photopolymer resins on a stereolithographic 3D printer. The use of low-cost biobased acrylates as the main component makes these resins potentially cost-competitive with respect to their commercial counterparts. Moreover, the bioresin formulations were successfully applied in a standardized SLA 3D printing process, thereby using the same procedure and settings as applied for commercial resins. The viscosity of the acrylate resin is an essential parameter in the 3D printing process and is controlled by the monomer to oligomer ratio. Typically, a shear rate of 100 s^{-1} is

achieved during the recoat of liquid resin in the printing process[14,15]. In this region, all bioresins have a viscosity below 5 Pa·s (**Figure 1**) and are appropriate for application in stereolithographic printing equipment.

Lithography-based additive manufacturing is recognized for its excellent surface quality and precision in comparison to FDM and selective laser sintering (SLS)[16,17]. This is clearly demonstrated by the photographic and microscopic images representing the complex shaped prototypes (**Figure 4**). To the contrary, the mechanical properties of produced parts are limited due to the limited choice of materials suited for the SLA process[18,19]. Acrylate systems in general show brittleness and poor impact resistance due to high crosslink density and inhomogeneous network architecture. Consequently, the materials 3D printed from the renewable acrylate resins have an ultimate strength of 2-8 MPa (**Figure 2**), which is lower in comparison to commercial products[12]. Nevertheless, optimization of the post-treatment, by varying the duration of washing, drying, curing and temperature of curing, leads to a significant improvement in mechanical performance (**Figure 3**).

Microscopic analysis reveals the high feature resolution and excellent surface finishing of the produced prototypes under high magnification (**Figure 4**). The serrated vertical edges of the helices arise from the layer-by-layer SLA printing process, in which the top of an exposed layer receives a larger UV dose compared to the back of a layer[8]. The cracks observed on the surface of the fabricated prototypes can result from shrinkage forces developed in the UV curing process. Shrinkage in acrylate systems is found to be inversely related to the resin viscosity[20,21]. Hence, the extent of cracking (**Figure 4**) is reduced when applying more viscous photoresins (**Figure 1**).

Disclosures

The authors have nothing to disclose.

Acknowledgements

This study was supported by GreenPAC Polymer Application Centre as part of Project 140413: "3D Printing in Production". We would like to acknowledge Albert Hartman, Corinne van Noordenne, Rens van Leeuwen, Anniek Bruins, Femke Tamminga, Jur van Dijken and Albert Woortman for facilitating the video shooting.

References

1. Van Wijk, A., van Wijk, I. *3D Printing with Biomaterials: Towards a Sustainable and Circular Economy.* IOS Press. Amsterdam. (2015).
2. Gross, B. C., Erkal, J.L., Lockwood, S.Y., Chen, C.,Spence, D.M. Evaluation of 3D Printing and Its Potential Impact on Biotechnology and the Chemical Sciences. *Analytical Chemistry.* **86**, 3240-3253 (2014).
3. Chia, H.N., Wu, B.M. Recent advances in 3D printing of biomaterials. *Journal of Biological Engineering.* **9**, 4 (2015).
4. Mechels, F.P.W., Feijen, J., Grijpma, D.W. A review on stereolithography and its applications in biomedical engineering. *Biomaterials.* **31**, 6121-6130, (2010).
5. Skoog, S.A., Goering, P.L., Narayan, R.J. Stereolithography in tissue engineering. *Journal of Materials Science: Materials in Medicine.* **25**, 845-856, (2014).
6. Bhatia, S.K., Ramadurai, K.W. *3D Printing and Bio-Based Materials in Global Health.* Springer. Cham. (2017).
7. Oskui, S. M., Diamante, G., Liao, C., Shi, W., Gan, J., Schlenk, D., Grover, W. H. Assessing and Reducing the Toxicity of 3D-Printed Parts. *Environmental Science & Technology Letters.* **3**, 1- 6 (2016).
8. Gong, H., Beauchamp, M., Perry, S., Woolley, A.T., Nordin, G.P. Optical approach to resin formulation for 3D printed microfluidics. *RSC Advances.* **5**, 106621-106632, (2015).
9. Zarek, M., Layani, M., Cooperstein, I, Sachyani, E., Cohn, D., Magdassi, S. 3D printing of shape memory polymers for flexible electronic devices. *Advanced Materials.* **28**, 4449-4454, (2016).
10. Ligon-Auer, S.C., Schwentenwein, M., Gorsche, C., Stampfl, J., Liska, R. Toughening of photo-curable polymer networks: A review. *Polymer Chemistry.* **7**, 257-286 (2016).
11. Miao, S., Zhu, W., Castro, N.J., Nowicki, M., Zhou, X., Cui, H., Fisher, J.P., Zhang, L.G. 4D printing smart biomedical scaffolds with novel soybean oil epoxidized acrylate. *Scientific Reports.* **6**, 27226, (2016).
12. Voet, V.S.D., Strating, T., Schnelting, G.H.M., Dijkstra, P., Tietema, M., Xu, J., Woortman, A.J.J., Loos, K., Jager, J., Folkersma, R. Biobased acrylate photocurable resin formulation for stereolithographic 3D printing. *ACS Omega.* **3**, 1403-1408 (2018).
13. Ligon-Auer, S.C., Liska, R., Stampfl, J., Gurr, M., Mülhaupt, R. Polymers for 3D Printing and Customized Additive Manufacturing. *Chemical Reviews.* **117**, 10212−10290, (2017).
14. Weng, Z., Zhou, Y., Lin, W., Senthil, T., Wu, L. Structure-property relationship of nano enhanced stereolithography resin for desktop SLA 3D printer. *Composites: Part A.* **88**, 234-242, (2016).
15. Scalera, F., Esposito Corcione, C., Montagna, F., Sannino, A., Maffezzoli, A. Development and characterization of UV curable epoxy/ hydroxyapatite suspensions for stereolithography applied to bone tissue engineering. *Ceramics International.* **40**, 15455-15462, (2014).
16. Lee, H., Fang, N. X. Micro 3D Printing using a digital projector and its application in the study of soft materials mechanics. *Journal of Visualized Experiments.* (69) e4457, (2012).
17. Huemer, K., Squirrell, J. M., Swader, R., Pelkey, K., LeBert, D. C., Huttenlocher, A., Eliceiri, K.W. Long-term live imaging device for improved experimental manipulation of zebrafish larvae. *Journal of Visualized Experiments.* (128), e56340, (2017).
18. Decker, C. Light-induced crosslinking polymerization. *Polymer International.* **51**, 1141−1150, (2002).
19. Elliot, J.E., Bowman, C.N. Predicting network formation of free radical polymerization of multifunctional monomers. *Polymer Reaction Engineering.* **10**, 1-19, (2002).
20. Ellakwa, A., Cho N., Lee, I.B. The effect of resin matrix composition on the polymerization shrinkage and rheological properties of experimental dental composites. *Dental Materials.* **23**, 1229-1235, (2007).

21. Charton, C., Falk, V., Marchal, P., Pla, F., Colon, P. Influence of *T*g, viscosity and chemical structure of monomers on shrinkage stress in light-cured dimethacrylate-based dental resins. *Dental Materials.* **23**, 1447-1459, (2007).